

Out-of-equilibrium quantum dynamics of fermionic gases in the presence of localized particle loss

Francesco Tarantelli and Ettore Vicari

Dipartimento di Fisica dell'Università di Pisa and INFN, Largo Pontecorvo 3, I-56127 Pisa, Italy

(Dated: May 10, 2022)

We address the effects of dissipative defects giving rise to a localized particle loss, in one-dimensional non-interacting lattice fermionic gases confined within a region of size ℓ . We consider homogeneous systems within hard walls and inhomogeneous systems where the particles are trapped by space-dependent external potentials, such as harmonic traps. We model the dissipative particle-decay mechanism by Lindblad master equations governing the time evolution of the density matrix. The resulting quantum dynamics is analyzed in protocols starting from the ground state of the Hamiltonian for N_0 particles, then evolving under the effect of one dissipative particle-loss defect, for example at the center of the system. We study the interplay between time, size ℓ and the number N_0 of initial particles, considering two different situations: (i) fixed number N_0 of initial particles; (ii) fixed ratio N_0/ℓ , corresponding to the *thermodynamic* limit of the initial equilibrium state. We show that the quantum evolutions of the particle number and density develop various intermediate and asymptotic dynamic regimes, and nontrivial large-time states when the dissipative mechanism acts at the center of the system.

I. INTRODUCTION

The progress in atomic physics and quantum technologies allows us to deepen our comprehension of the coherent quantum dynamics of the many-body systems [1, 2], and its interplay with dissipative mechanisms arising from the interaction with the environment [3–9], either due to unavoidable incoherent mechanisms, or suitably engineered system-bath couplings. This opens the road to the investigation of dissipation-driven phenomena, which may show the emergence of new collective behaviors, such as novel quantum phases and phase transitions driven by dissipation [10–14], peculiar behaviors in the low-dissipative regime [15–22], for example dynamic scaling at quantum transitions [23]. Several studies have also addressed localized dissipative mechanisms in many-body systems, see e.g. Refs. [24–53].

In this paper we address the effects of localized particle-loss defects in lattice fermionic gases confined in a space region of size ℓ . We consider quantum systems where particles are constrained within hard walls, and systems where they are confined by a space-dependent potential, such as an effective harmonic potential. These particle systems are relevant for experimental setups, for example in cold-atom experiments [54], where a finite number of atoms is confined within a limited spatial region, typically by effectively harmonic potentials, or by effective hard walls, as experimentally realized in Ref. [55]. Within this class of confined systems, we investigate the dynamic features arising from localized particle-loss dissipative mechanisms, which may be controllable or inevitably present in the experiments.

For this purpose, we consider dynamic finite-size scaling (FSS) frameworks, which have been particular effective to the investigation of thermal and quantum phase transitions, see e.g. Refs. [23, 56–58]. This approach allows us to characterize the dynamics in the presence of localized particle-loss dissipation, identifying different

dynamic regimes related to different features of the dissipative system, whose time scales are associated with powers of the size ℓ . To achieve quantitative information on the behavior of particle systems of finite (relatively large) size, we consider two different large-size FSS limits: (i) the dynamic FSS limit keeping the initial number N_0 of particles fixed (before activating the particle-loss mechanism); (ii) the case in which the ratio N_0/ℓ^d (for d spatial dimensions) is kept fixed, corresponding to a nonzero chemical potential. The corresponding scaling laws provide complementary information on the actual dynamics of finite-size systems with a relatively large size.

As paradigmatic models we consider one-dimensional lattice models of non-interacting spinless fermionic gases, within hard-wall and harmonic traps, subject to dissipative perturbations that give rise to a particle loss localized at one of the sites of the lattice, such as the set up sketched in Fig. 1. We model the dissipative particle-decay mechanism by Lindblad master equations governing the time evolution of the density matrix [59–63]. To investigate the effects of the localized particle-loss dissipation, we study the quantum dynamics arising from protocols starting from the ground state of the fermionic gas, then evolving under the effect of the particle-loss dissipation, for example localized at the center of the system. This is analyzed in the large- ℓ limit for two different initial conditions: fixed number N_0 of initial particles and fixed ratio N_0/ℓ , which corresponds to the *thermodynamic* limit of the initial fermionic gases at equi-

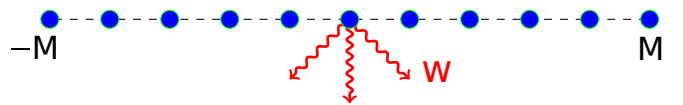


FIG. 1: Sketch of a fermionic chain of size $L = 2M + 1$ subject to a localized particle loss at the central site, with strength controlled by the dissipation parameter w .

librium, in both hard walls and harmonic traps. The quantum evolution of the particle number and space-dependent density turns out to develop various dynamic scaling regimes, and nontrivial large-time behaviors when the dissipative mechanism acts at the center of the system.

Some issues concerning the behavior of fermionic gases in the presence of localized dissipative interactions have been already discussed in Refs. [35, 36, 39, 42, 43, 49], mainly for homogeneous systems neglecting boundary effects. Here we extend these studies by analyzing the interplay between time, size of the system, and number N_0 of initial particles. We analyze the various large-time and intermediate dynamic regimes, in both homogeneous particle systems within hard walls and inhomogeneous particle systems in harmonic traps. Substantially different and peculiar behaviors are observed in fermionic gases confined by hard walls and harmonic traps.

The understanding of the interplay between the time dependence and the finite size of the system is essential to interpret results in various experimental contexts. For example this issue is fundamental for small-size quantum simulators operating on a limited amount of quantum objects, in the presence of controlled dissipation. We also mention experiments with cold atoms within a trap of finite size, when the many-body correlations become eventually sensitive to the trapping potential (local density approximations generally fail to describe quantum correlations, in particular when they are critical [64] and/or out-of-equilibrium [23]).

The paper is organized as follows. In Sec. II we present the models of spinless fermionic gases confined within hard walls or traps arising from external power-law potentials, the description of the localized particle-loss dissipation, the dynamic protocols that we consider to study the dissipative effects, and the main equations that allow us to study the evolution of the particle number and density. In Sec. III we present results for fermionic gases confined within hard walls, discussing the main features of the asymptotic stationary states, and the emerging dynamic scaling behaviors characterizing the quantum evolution arising from the protocols. In Sec. IV we focus on fermionic gases within harmonic traps, showing again the emergence of various dynamic regimes. Finally, in Sec. V we summarize and draw our conclusions.

II. FREE LATTICE FERMIONS WITH LOCALIZED DISSIPATIVE DEFECTS

A. The Hamiltonian

We consider one-dimensional N -particle Fermi gases defined on a chain with $L = 2M + 1$ sites, by the Hamiltonian

$$\hat{H} = -\kappa \sum_{x=-M}^{M-1} (\hat{c}_x^\dagger \hat{c}_{x+1} + \hat{c}_{x+1}^\dagger \hat{c}_x), \quad (1)$$

where \hat{c}_x is a fermion one-particle operator, and $\hat{n}_x = \hat{c}_x^\dagger \hat{c}_x$ is the particle density operator. We consider hard-wall (open) boundary conditions. The site $x = 0$ is the central site of the chain. In the following we set $\hbar = 1$, $\kappa = 1$, and the lattice spacing $a = 1$, from which one can easily derive the units of all other dimensionful quantities considered in the rest of the paper.

We also consider fermionic systems where the particles are trapped by an external potential, which can be taken into account by adding a corresponding term to the Hamiltonian (1), such as

$$\hat{H}_t = - \sum_x (\hat{c}_x^\dagger \hat{c}_{x+1} + \hat{c}_{x+1}^\dagger \hat{c}_x) + \sum_x V(r) \hat{n}_x, \quad (2)$$

where

$$\hat{n}_x = \hat{c}_x^\dagger \hat{c}_x, \quad V(r) = (r/L_t)^p, \quad r \equiv |x|, \quad (3)$$

p is a positive number, r is the distance from the center $x = 0$ of the trap, and L_t plays the role of trap size.¹ The trapping potential is effectively harmonic in most cold-atom experiments [54], i.e., $p = 2$. In the limit $p \rightarrow \infty$ we recover the model (1) with hard-wall boundary conditions and $M = \lfloor L_t \rfloor$. The size of systems described by the Hamiltonian \hat{H}_t with finite p is supposed to be infinite. However for practical purposes it is sufficient to consider models within hard walls with $L \gg L_t$. Indeed the large-size convergence is generally fast for sufficiently large values of p , including $p = 2$, due to the fact that the average particle density $\langle \hat{n}_x \rangle$ vanishes rapidly for $|x| \gg L_t$. The main features of the behavior of fermionic gases trapped by a inhomogeneous external power-law potentials have been much investigated, see e.g. Refs. [66–74].

In systems within both hard-wall and inhomogeneous traps, the particle number operator

$$\hat{N} = \sum_x \hat{n}_x \quad (4)$$

commutes with both Hamiltonians (1) and (2). Therefore the particle number is conserved in both cases. In the following we consider ground states for a number N_0 of particles as starting point of dynamic protocols involving dissipative mechanisms.

B. Localized particle-decay dissipation

We model the dissipative mechanisms within the Lindblad framework [59, 60], where the evolution of the ma-

¹ L_t plays the role of trap size [54, 65, 66], so that the *thermodynamic* limit is obtained in the large trap-size limit, $L_t \rightarrow \infty$, keeping the ratio between the particle number N and the trap size L_t constant, which can be equivalently obtained by adding a chemical-potential term in the Hamiltonian, such as the one reported in Eq. (16).

trix density $\rho(t)$ of the system is described by the equation [61, 62]

$$\frac{\partial \rho}{\partial t} = \mathcal{L}[\rho] = -i [\hat{H}, \rho] + \mathbb{D}[\rho]. \quad (5)$$

We recall that the conditions leading to the Lindblad framework are typically satisfied in quantum optical implementations [9, 63]. The form of the operator $\mathbb{D}[\rho]$ depends on the nature of the dissipation arising from the interaction with the bath. We consider a localized particle-decay dissipation acting at the site z , modeled by the Lindblad operator [17, 23, 42, 43, 63, 75–77]

$$\mathbb{D}[\rho] = w \left[\hat{c}_z \rho \hat{c}_z^\dagger - \frac{1}{2} (\rho \hat{c}_z^\dagger \hat{c}_z + \hat{c}_z^\dagger \hat{c}_z \rho) \right], \quad (6)$$

where w is a parameter controlling the strength of the particle-loss dissipation.

The reflection symmetry with respect to the center of the confined particle system is only preserved when the particle loss is localized at the center. As we shall see, this will lead to peculiar behaviors with respect to the case of particle-loss dissipation localized at generic sites.

The approach to the asymptotic stationary states are generally controlled by the Liouvillian gap $\Delta_{\mathcal{L}}$ associated with the generator \mathcal{L} entering the Lindblad equation (5) [12, 33, 41, 61, 62]. The asymptotic stationary state is provided by the eigenstate of \mathcal{L} with vanishing eigenvalue, $\Lambda_0 = 0$, while all other eigenstates have eigenvalues Λ_i with negative real part, i.e. $\text{Re} \Lambda_i < 0$ for any $i > 0$.

C. Dynamic protocol

To study fermionic gases under the effects of a localized particle-loss mechanism, we consider the following dynamic protocol, for systems within both hard-wall and harmonic traps, respectively of size $L = 2M + 1$ and L_t .

- The protocol starts at time $t = 0$ from the ground state of the Hamiltonian (1) or (2) with a number N_0 of particles. We recall that the ground state of N_0 noninteracting fermionic particles is obtained by filling the lowest N_0 one-particle energy levels.
- The time evolution for $t > 0$ is driven by the Lindblad equation (5) for the density matrix $\rho(t)$, with particle-decay dissipation localized at a site z and controlled by the parameter w .
- The particle density and total particle number,

$$n_x(t) = \text{Tr}[\rho(t)\hat{n}_x], \quad N(t) = \text{Tr}[\rho(t)\hat{N}], \quad (7)$$

are monitored during the out-of-equilibrium evolution for $t > 0$, up to their large-time behaviors.

To compute the particle density $n_x(t)$ and particle number $N(t)$, we proceed as follows. We introduce the correlation functions

$$\mathcal{C}_{x,y}(t) = \text{Tr}[\rho(t) \hat{c}_x^\dagger \hat{c}_y]. \quad (8)$$

For homogeneous systems described by the Hamiltonian (1), the Lindblad equation (5) implies

$$\begin{aligned} \frac{d\mathcal{C}_{x,y}}{dt} &= i(\mathcal{C}_{x,y+1} - \mathcal{C}_{x-1,y} + \mathcal{C}_{x,y-1} - \mathcal{C}_{x+1,y}) \\ &\quad - \frac{w}{2}(\delta_{z,y} + \delta_{x,z})\mathcal{C}_{x,y}, \end{aligned} \quad (9)$$

where $\delta_{x,x} = 1$ and $\delta_{x,y} = 0$ for $x \neq y$. Since we consider open (hard-wall) boundary conditions, $\mathcal{C}_{xy}(t) = 0$ when the coordinates x or y refer to sites outside the space interval $[-M, M]$. An analogous equation can be derived in the presence of an inhomogeneous external trapping potential, cf. Eq. (2). We obtain

$$\begin{aligned} \frac{d\mathcal{C}_{x,y}}{dt} &= i(\mathcal{C}_{x,y+1} - \mathcal{C}_{x-1,y} + \mathcal{C}_{x,y-1} - \mathcal{C}_{x+1,y}) \\ &\quad + i \frac{|x|^p - |y|^p}{L_t^p} \mathcal{C}_{x,y} - \frac{w}{2}(\delta_{z,y} + \delta_{x,z})\mathcal{C}_{x,y}. \end{aligned} \quad (10)$$

Then, after numerically solving the above equations, we use the relations

$$n_x(t) = \mathcal{C}_{x,x}(t), \quad N(t) = \sum_x n_x. \quad (11)$$

One can easily check that for both hard-wall and harmonic traps the derivative of the particle number is proportional to the average particle density n_z at the site z where the particle-decay dissipation is localized, i.e.

$$\frac{dN(t)}{dt} = -w n_z(t) < 0. \quad (12)$$

Therefore the particle number decays monotonically, since $n_z(t) \geq 0$, and the particle loss stops if $n_z(t) = 0$ asymptotically.

One may also consider the energy of the system, defined as

$$E(t) = \text{Tr}[\rho(t)\hat{H}], \quad (13)$$

for which the Lindblad equation implies

$$\frac{dE(t)}{dt} = \text{Tr} \left[\frac{d\rho(t)}{dt} \hat{H} \right] = w \text{Tr}[\mathbb{D}[\rho] \hat{H}]. \quad (14)$$

For systems with particle-loss dissipation localized at the central site $x = 0$, we obtain

$$\frac{dE(t)}{dt} = w \text{Re}(\mathcal{C}_{0,1} + \mathcal{C}_{-1,0}) = 2w \text{Re} \mathcal{C}_{0,1}, \quad (15)$$

which holds for systems within hard walls and also inhomogeneous traps.

III. FERMI GASES WITHIN HARD WALLS

In this section we consider homogeneous Fermi chains, cf. Eq. (1), and discuss the dynamic evolution under the particle-loss dissipation described by the Lindblad equation (5), in particular Eq. (9). For this purpose, we numerically solve the differential equation (9) using the fourth-order Runge-Kutta method (with an accuracy of approximately 10^{-8} on the evolution of the particle number).

We study the interplay between the time dependence, the number N_0 of initial particles and the size $L = 2M + 1$ of the lattice. For this purpose we consider two different situations: (i) the number N_0 of particles is kept fixed while increasing M ; (ii) the number of particles is increases as $N_0 \sim M$, so that the ratio N_0/M fixed, while increasing M . Note that the latter condition can be equivalently realized in the large-size limit by adding a chemical potential to the Hamiltonian (1), i.e.

$$\hat{H}_\mu = -(\mu + 2) \sum_x \hat{n}_x. \quad (16)$$

The value $\mu = \mu_{vs} = -2$ corresponds to the vacuum-superfluid transition point [67, 78], separating the phase where the lowest Hamiltonian eigenstate has $N = 0$ particles from the one for $\mu > -2$ where the ground-state has $N \sim L$ fermions.

In the following we first analyze the asymptotic large-time regime. Then we show that the time dependence of the particle number develops various asymptotic and intermediate regimes, which may differ in the cases we keep N_0 or N_0/M fixed.

A. Asymptotic stationary states

For generic locations of the particle-loss defects, the asymptotic stationary state turns out to be trivial, i.e. an empty state without particles. However in some cases, in particular when the defect is localized at the center of the chain, the quantum evolution of the system keeps a residual number of particles even in the large-time limit.

This can be shown analytically, straightforwardly extending the analysis for non-interacting bosons reported in Ref. [29], to free fermions. Since we are considering systems of size $L = 2M + 1$ with hard-wall boundary conditions, we introduce the fermionic operators

$$\hat{\eta}_k = \sqrt{\frac{2}{L+1}} \sum_{y=1}^L \sin\left(\frac{\pi ky}{L+1}\right) \hat{c}_y, \quad (17)$$

where, to simplify the formulas, we have shifted the coordinates so that $y = x + M + 1$ (therefore the site coordinates are $y = 1, \dots, L$, and the center is located at $y = M + 1$). This allows us to write the Hamiltonian (1)

as

$$\hat{H} = -2 \sum_{k=1}^L \cos\left(\frac{\pi k}{L+1}\right) \hat{n}_k, \quad \hat{n}_k = \hat{\eta}_k^\dagger \hat{\eta}_k. \quad (18)$$

The operator \hat{n}_k commutes with the Hamiltonian, i.e. $[\hat{H}, \hat{n}_k] = 0$, and satisfies $\sum_k \hat{n}_k = \hat{N} = \sum_x \hat{n}_x$. Its expectation value

$$n_k(t) = \text{Tr}[\rho(t) \hat{n}_k] \quad (19)$$

counts the number of particles associated with the mode k . The initial equilibrium ground state with N_0 fermionic particles is constructed by filling the first N_0 one-particle energy levels, thus at $t = 0$ we have $n_k = 1$ for $k \leq N_0 \leq L$, and zero otherwise. The modes with odd (even) k are even (odd) under inversion with respect to the center $y = M + 1$ of the chain. The time evolution of n_k is determined by the Lindblad equation for the density matrix. Considering a particle-decay dissipation located at a generic site z , straightforward calculations lead to the equation

$$\begin{aligned} \frac{dn_k}{dt} &= -\frac{w}{L+1} \sin\left(\frac{\pi kz}{L+1}\right) \\ &\times \sum_{q=1}^L \sin\left(\frac{\pi qz}{L+1}\right) \text{Tr}[\rho(t) (\hat{\eta}_q^\dagger \hat{\eta}_k + \eta_k^\dagger \hat{\eta}_q)], \end{aligned} \quad (20)$$

where, due to the fact that $[\hat{H}, \hat{n}_k] = 0$, the only contribution to the time derivative of n_k comes from the dissipative term. We note that the r.h.s. of Eq. (20) vanishes when

$$kz = j(L+1), \quad j = 1, 2, \dots, \quad (21)$$

thus implying the conservation of the corresponding particle number n_k even in the presence of localized particle-decay dissipation.

If we consider a central-site dissipation, thus $z = M + 1 = (L + 1)/2$ [we recall that we are using shifted coordinates with respect to Eq. (1)], then the condition (21) reduces to $k = 2j$, thus implying that n_k remains unchanged for all even k (whose odd-parity modes vanish at the central dissipative site), while it gets suppressed for odd k . Therefore, Eq. (20) implies that half of the fermions survives centrally localized decay dissipation. More precisely the stationary states are characterized by a residual particle number $N_{\text{asy}} = N_0/2$ for even N_0 , and $N_{\text{asy}} = (N_0 - 1)/2$ for odd N_0 .

Note that the particle loss localized at the center, preserving the parity symmetry with respect to the center of the chain, is the optimal one to keep a fraction of fermionic particles at large time. For example, in the case of a dissipation at the boundaries, i.e., when $z = 1$ or $z = M$ in Eq. (20), no particles survive because all k -modes are involved by the Lindblad operator, leading to the complete suppression of the particles filling the initial ground state.

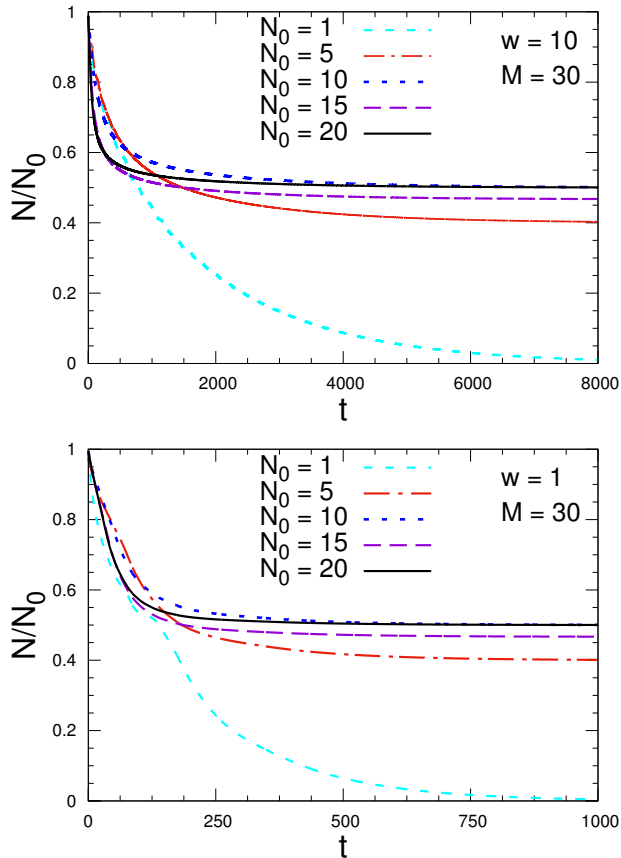


FIG. 2: Behavior of the ratio $N(t)/N_0$ for the central-site particle-loss dissipation in systems of size $L = 61$ ($M = 30$) within hard walls, various initial particle number N_0 , and dissipation localized at the center of the system, with $w = 1$ (bottom) and $w = 10$ (top). In both cases asymptotic stationary limit turns out to converge to $N/N_0 = 1/2$ for even N_0 , and $N/N_0 = (N_0 - 1)/(2N_0)$ for odd N_0 . Note that approach to the asymptotic value is slower for $w = 10$ than $w = 1$.

The above analytical results are confirmed by the numerical results for the central particle-loss dissipation, see for example Fig. 2 where we show the time dependence of the ratio $N(t)/N_0$ for various values of N_0 and w , and in particular the approach to its nonzero asymptotic limit. Also the space dependence of the particle density n_x turns out to become stable asymptotically, approaching a stationary configuration, as shown in Fig. 3. In Fig. 4 we show some results for the spatial dependence of the average particle density n_x of the asymptotic stationary states. We note that n_x is quite flat except at $x = 0$ where the dissipative mechanism acts, and at the boundaries of the chain (essentially due to the hard-wall boundary conditions). The almost flat region shows some spatial oscillations, which appear suppressed when $N_0 \approx M$ and $N_0 \approx 2M$.

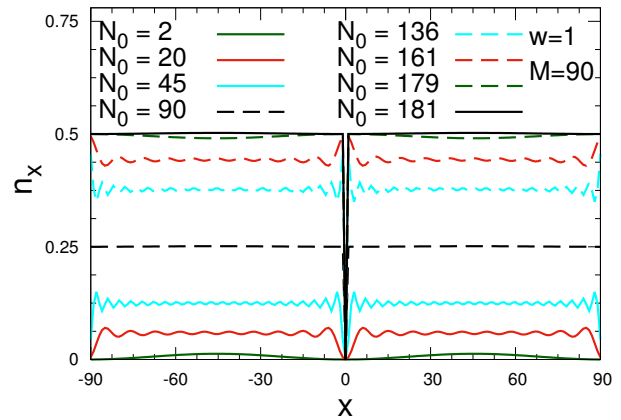


FIG. 3: Data for the quantum evolution of the fermionic gas within hard walls, size $L = 2M + 1$ with $M = 90$, initial particle number $N_0 = 10$, dissipation localized at the center of the chain with $w = 1$. We show the particle density $n_x(t)$ at the sites $x = 0$ and $x = 10$ (top), and the ratio $N(t)/N_0$ (bottom). They approach asymptotic stationary limits (at least within the numerical precision, which is very accurate).

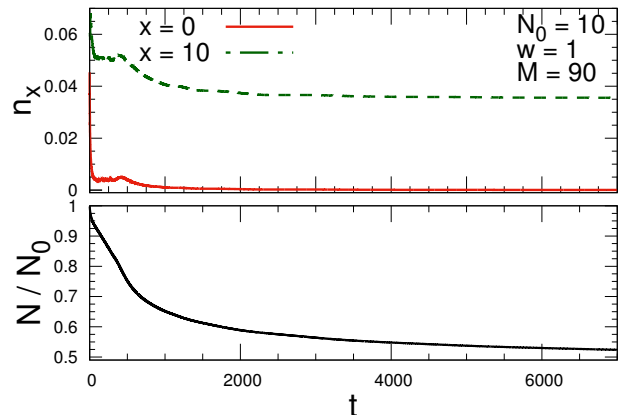


FIG. 4: Asymptotic stationary limit of the particle density n_x for systems of size $L = 181$ ($M = 90$) within hard-wall boundary conditions, in the presence of a central-site dissipation with $w = 1$, and for various N_0 . In all cases the particle density vanishes for $x = 0$, and it is almost flat elsewhere, apart from small spatial oscillations, which appear similar to the Friedel oscillations characterizing the behavior of closed particle systems.

B. Approach to the asymptotic states

1. Large-size behavior of the Liouvillian gap

The approach to the stationary state is controlled by the Liouvillian gap $\Delta_{\mathcal{L}}$ of the generator \mathcal{L} of the Lindblad equation [12, 33, 41, 61, 62],

$$\Delta_{\mathcal{L}} = -\text{Max}_{i>0} \text{Re}(\Lambda_i), \quad (22)$$

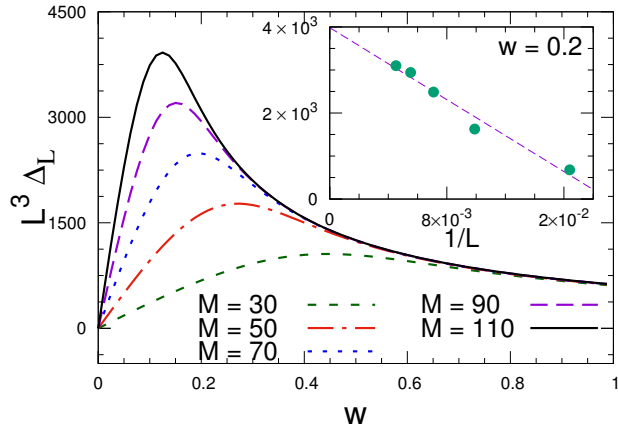


FIG. 5: The Liouvillian gap $\Delta_{\mathcal{L}}$ for particle-decay dissipation localized at the center of the chain, for various system size $L = 2M + 1$. The curves appear to converge with increasing M ; this is clearly shown at least for $w \gtrsim 0.2$, as also shown by the large- L convergence at a fixed value $w = 0.2$ [suggesting that the corrections to the asymptotic scaling behavior (23) are approximately $O(L^{-1})$]. We conjecture that the convergence extends to any $w > 0$, but it is nonuniform when decreasing w toward zero, see text.

where Λ_i are the eigenvalues of \mathcal{L} (we recall that the largest eigenvalue is $\Lambda_0 = 0$ and $\text{Re } \Lambda_i < 0$ for any $i > 0$). The Liouvillian gap for homogeneous spin chains and fermionic wires with localized dissipative mechanisms, such as that described by Eq. (6), shows generally the asymptotic finite-size behavior [25, 26, 33, 41, 48]

$$\Delta_{\mathcal{L}}(w, L) \approx D_{\mathcal{L}}(w) L^{-3}. \quad (23)$$

We expect that this asymptotic large- L behavior holds independently of the location of the particle-decay dissipation, and it does not depend on the initial conditions, thus on N_0 . The scaling equation (23) implies that the approach to the asymptotic behavior becomes slower and slower with increasing the size L of the lattice at fixed w .

The asymptotic behavior (23) is confirmed by numerical analyses of the Liouvillian gap using the method outlined in Ref. [25], see App. A. Some numerical results are shown by Figs. 5 and 6, for particle-decay dissipation localized at the center and at the boundary of the chain, respectively.

In both cases, $\Delta_{\mathcal{L}}$ appears nonmonotonic, increasing for small values of w and decreasing for sufficiently large dissipation strength w , for any L . The approach to the asymptotic behavior becomes slower and slower with increasing w for large w . In particular, $\Delta_{\mathcal{L}}(w, L)$ shows the large- w behavior $L^3 \Delta_{\mathcal{L}}(w) \approx D_{\mathcal{L}}(w) \sim w^{-1}$. This explains the results shown in Fig. 2, where the approach to the asymptotic value of the particle number for $w = 10$ turns out to be slower than that for $w = 1$. The suppression in the limit of strong dissipation, for large w , may be interpreted as a quantum-Zeno-like phenomenon [79, 80], where a strong dissipation somehow slows down the dy-

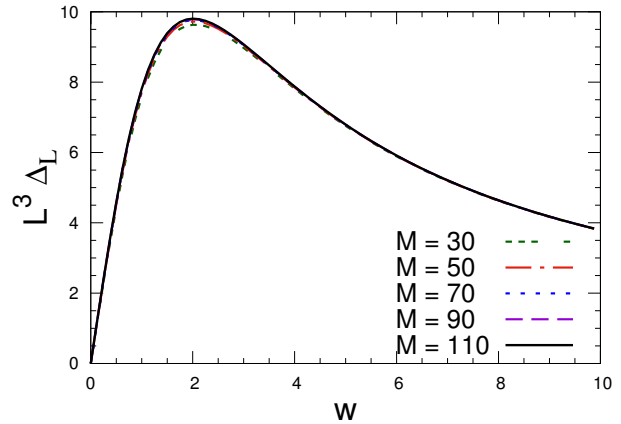


FIG. 6: Scaling behavior of the Liouvillian gap $\Delta_{\mathcal{L}}$ for particle-decay dissipation localized at one of the boundaries of the chain.

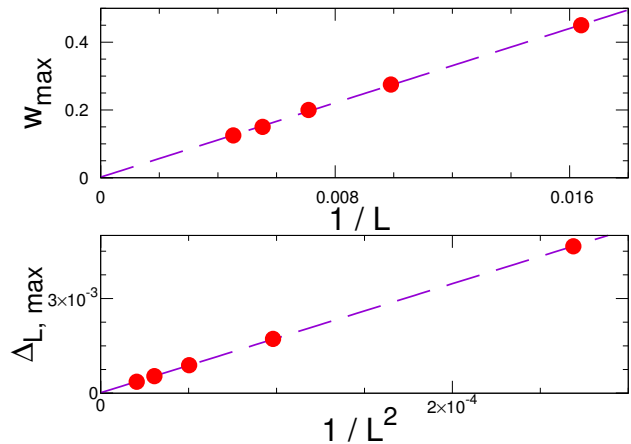


FIG. 7: Some details of the behavior of the Liouvillian gap $\Delta_{\mathcal{L}}$ for dissipation localized at the center of the lattice. We show the location w_{\max} of the maximum of the Liouvillian gap (top), showing that $w_{\max} \sim L^{-1}$, and value of $\Delta_{\mathcal{L}}$ at the maximum (bottom), showing that $\Delta_{\mathcal{L}}(w_{\max}) \sim L^{-2}$.

namics, see e.g. Refs. [45, 81] for the emergence of similar quantum Zeno regimes.

As shown by Figs. 5 and 6, the Liouvillian gap at fixed L has a maximum at an intermediate value of w . The corresponding values w_{\max} and $L^3 \Delta_{\mathcal{L}}(w_{\max})$ appears to rapidly converge to the large- L for dissipations localized at the boundaries. The approach to the asymptotic L^{-3} behavior (23) appears significantly slower in the case of dissipation localized at the center. The curves for different lattice sizes appear to converge for $w \gtrsim 0.2$, see Fig. 5 and in particular its inset. We conjecture that, like the case of dissipation at the boundaries, the convergence in the large-size limit extends to any $w > 0$, but it is nonuniform when decreasing w toward zero (i.e. the correction diverges for $w \rightarrow 0$). This is also supported by the plots reported in Figs. 7, which show that the location of the maximum value of the Liouvillian gap for central dissi-

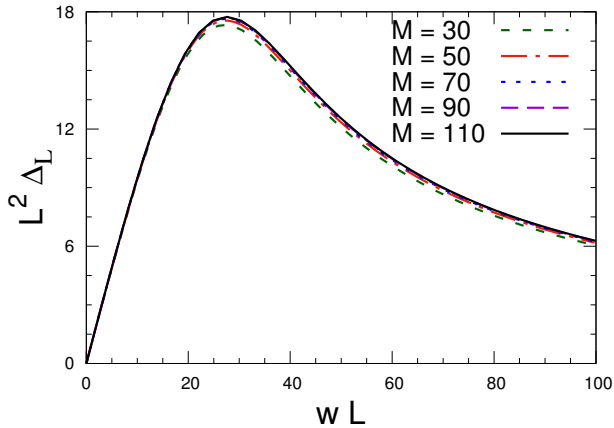


FIG. 8: Plots of $L^2 \Delta_{\mathcal{L}}$ versus wL for systems within hard walls and with central particle-loss dissipation, for various $L = 2M + 1$. They support the scaling equation (24).

pation moves toward $w = 0$, with $w_{\max} \sim L^{-1}$, and its maximum value decreases as $\Delta_{\mathcal{L}}(w_{\max}) \sim w_{\max}^2 \sim L^{-2}$, instead of the general asymptotic L^{-3} behavior for $w > 0$ fixed. Actually, they suggest that the Liouvillian gap for central dissipation shows also the asymptotic scaling behavior

$$\Delta_{\mathcal{L}}(w, L) \approx \mathcal{D}_{\mathcal{L}}(wL) L^{-2}, \quad (24)$$

obtained in the large- L limit keeping wL constant. This scaling behavior is demonstrated by the plot reported in Fig. 8. Therefore the function $\mathcal{D}_{\mathcal{L}}(w)$ entering the asymptotic L^{-3} behavior (23) must be singular for $w \rightarrow 0$ in the case of central-site dissipation, diverging as w^{-1} .

Note that the above considerations on the behavior of the Liouvillian gap apply to generic values of w , and, of course, they do not depend on the initial number N_0 of particles. In the following we will mainly present results for the value $w = 1$ of the dissipation parameter, whose dynamic scenarios are shared with those arising from generic finite values of w .

2. Large-time behavior of the particle number

On the basis of the large-size behavior of the Liouvillian gap, we expect that the time scale t_a of the approach to the stationary state is given as

$$t_a \sim \Delta_{\mathcal{L}}^{-1} \sim L^3, \quad (25)$$

at fixed $w > 0$. This time scale must characterize the approach to the stationary limits of the particle number and density. This is confirmed by the numerical computations, see for example Fig. 9 where we report results for the ratio

$$R_N(t) \equiv \frac{N(t) - N_{\text{asy}}}{N_0 - N_{\text{asy}}}, \quad (26)$$

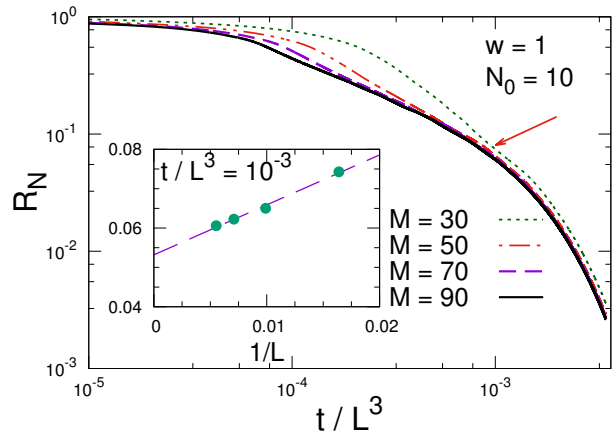


FIG. 9: The time dependence of the ratio R_N versus t/L^3 ($L = 2M + 1$), for homogeneous systems within hard walls with $N_0 = 10$ and central particle-loss dissipation with $w = 1$. The data for various sizes M show clearly the convergence toward a dynamic scaling curve, approximately as $1/L$ as shown by the inset for a particular value of the ratio t/L^3 (the one indicated by the arrow in the main figure).

for protocols starting from a fixed number N_0 of particles. They show the asymptotic large- L scaling behavior

$$R_N(t, w, L) \approx A(t/L^3, w), \quad (27)$$

which also implies

$$\frac{dR_N(t, w, L)}{dt} \approx L^{-3} B(t/L^3, w).$$

As usual within FSS frameworks, the above asymptotic FSS behaviors are expected to hold in the large- L limit keeping the ratio t/L^3 and w fixed.

Analogous results are obtained for the case we start from a fixed ratio N_0/M (we recall that $L = 2M + 1$), as shown in Fig. 10 for $N_0/M = 1/2$, where we plot $N(t) - N_{\text{asy}}$ versus t/L^3 and the curves appear to collapse in the large- M limit. Note that when N_0/M is kept fixed, the quantity R_N defined in Eq. (26) is not appropriate, because it is always suppressed in the large-time limit, due to the denominator that behaves as $N_0 - N_{\text{asy}} \sim L$.

As we will show below, this is not the end of the story, indeed further peculiar intermediate scaling behaviors emerge, differing between the cases N_0 and N_0/M fixed.

C. Intermediate scaling behaviors keeping N_0 fixed

We now look for intermediate regimes of the time evolution, somehow associated with the time scales of the Hamiltonian (1) driving the unitary dynamics, and therefore to its gap Δ_H , i.e. the energy difference between the first excited state and the ground state. When keeping the particle number N_0 fixed, Δ_H behaves asymptotically as $\Delta_H \sim L^{-2}$, corresponding to the dynamic exponent $z = 2$ of the vacuum-superfluid transition [78].

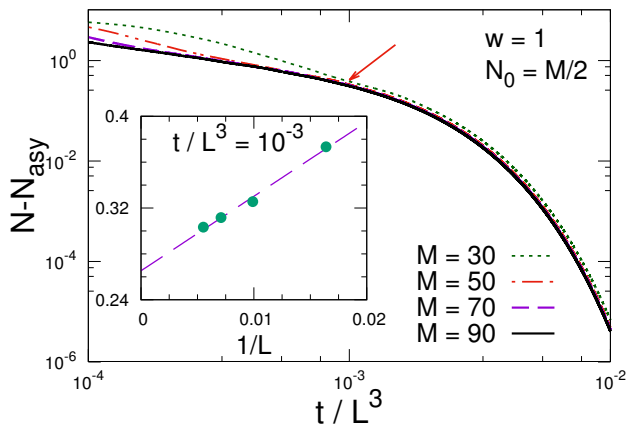


FIG. 10: The difference $N(t) - N_{\text{asy}}$ vs t/L^3 , for systems within hard walls with $N_0/M = 1/2$, and central dissipation with $w = 1$. Again we observe the asymptotic convergence toward a dynamic scaling curve, as shown by the inset for a particular value of t/L^3 (indicated by the arrow in the main figure).

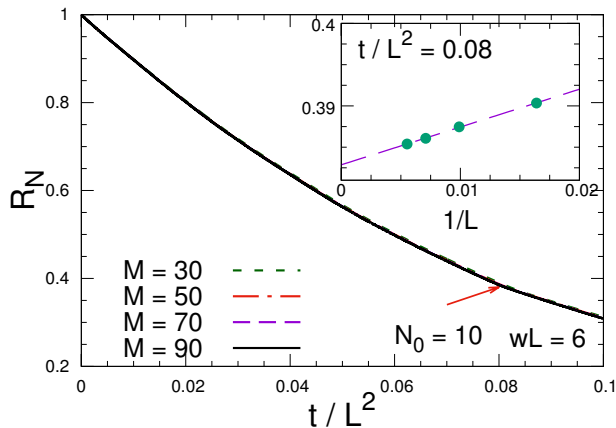


FIG. 11: The ratio R_N versus t/L^2 for systems within hard walls with $N_0 = 10$, central dissipation with $wL = 6$, for various lattice sizes $L = 2M + 1$. The data appear to converge toward a scaling curve in the large- L limit, as demonstrated by the data reported in the inset for a particular value of the ratio t/L^2 .

We want to check whether the out-of-equilibrium dynamics develops an intermediate regimes somehow controlled by the Hamiltonian driving of the Lindblad equation, whose intrinsic time scale is related to its gap, i.e. $t \sim \Delta_H^{-1} \sim L^2$, which is much smaller than the time scale $t \sim L^3$ characterizing the approach to the stationary large-time limit (of course, for sufficiently large L , and in particular in the large- L limit). As we shall see, a closer look at the time evolution provides a clear evidence of such an intermediate regime, which also requires a rescaling of the dissipation strength, thus it emerges only at small values of w .

In Fig. 11 we show some results for the time depen-

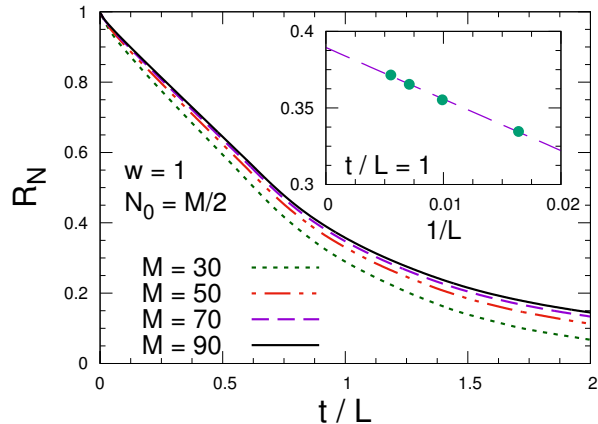


FIG. 12: Behavior of the ratio R_N versus t/L , for systems within hard walls with $N_0/M = 1/2$, and central dissipation with $w = 1$. The inset shows the $1/L$ approach to the large- L asymptotic behavior.

dence of the particle number in the case of systems with central-site dissipation starting from a fixed number of particles. We observe that the above-mentioned intermediate regime exists, and extends to any $t \sim L^2$, if we perform an appropriate rescaling of the dissipation parameter w , decreasing w as $w \sim L^{-1}$. Indeed the numerical results clearly support the large- L scaling behavior

$$R_N(t, w, L) \approx U(t/L^2, wL), \quad (28)$$

which corresponds to another FSS limit, obtained by increasing L keeping the ratio t/L^2 and the product wL fixed. Note that this intermediate scaling behavior is expected to hold even for large values of the ratio t/L^2 , because it is also compatible with the alternative scaling behavior (24) of the Liouvillian gap.

D. Intermediate dynamic behavior keeping N_0/M fixed

We now consider the large- L behavior in the case we keep the ratio N_0/M fixed when increasing $L = 2M + 1$. This corresponds to the superfluid phase, i.e. when the chemical potential μ is larger than that at the vacuum-superfluid transition, $\mu > -2$. Within the superfluid phase, the gap Δ_S of isolated free Fermi gases behaves as [78] $\Delta_S \sim L^{-1}$.

Again we want to check whether the out-of-equilibrium dynamics in this condition develops an intermediate regime controlled by the part of the Lindblad equation driving the unitary dynamics introduces a time scale $t \sim \Delta_S^{-1} \sim L$ (again, much smaller than the time scale $t \sim L^3$ characterizing the approach to the stationary large-time limit). Like the case at fixed N_0 , we show that such an intermediate regime exists, without tuning w toward zero.

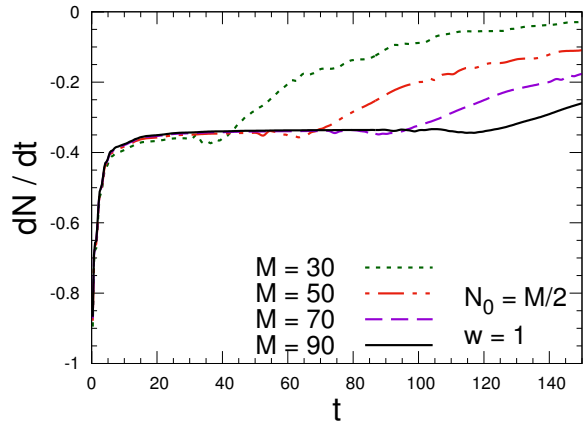


FIG. 13: The time dependence of the derivative of the particle number, for systems within hard walls with central-site dissipation with $w = 1$, starting from ground states with $N_0/M = 1/2$ fixed.

The existence of a corresponding intermediate regime of the dynamics is demonstrated by the results shown in Fig. 12, leading to the intermediate FSS ansatz

$$R_N(t, w, L) \approx W(t/L, w), \quad (29)$$

obtained keeping t/L fixed in the large- L limit.

We finally report the existence of a further early-time regime when we start from the ground state for $N_0 \propto M$, as already noted in Ref. [43]. Indeed, for sufficiently small time

$$\frac{dN(t, w, L)}{dt} \approx f(t, w), \quad (30)$$

without showing any asymptotic size dependence. This is shown by the curves reported in Fig. 13. The behavior (30) is observed in the large-size limit, and can be considered as the *thermodynamic* limit of the quantum evolution, when the time is sufficiently small that the dynamics does not yet detect the effects of the boundaries. Indeed deviations are observed for $t \propto M$, thus later and later for larger and larger systems. At the end of this early-time regime, the intermediate regime (29) begins.

IV. FERMIONIC GASES WITHIN HARMONIC TRAPS

We now present results for lattice fermionic systems within traps arising from inhomogeneous external potentials, such as those in Eq. (3), in the presence of a particle-decay dissipation at the center of the trap, as described by the Lindblad equations (5) and (6). As already mentioned in the introduction, effective harmonic trapping mechanisms are quite common in cold-atom experiments [54]. Therefore their analysis is also relevant from a phenomenological point of view.

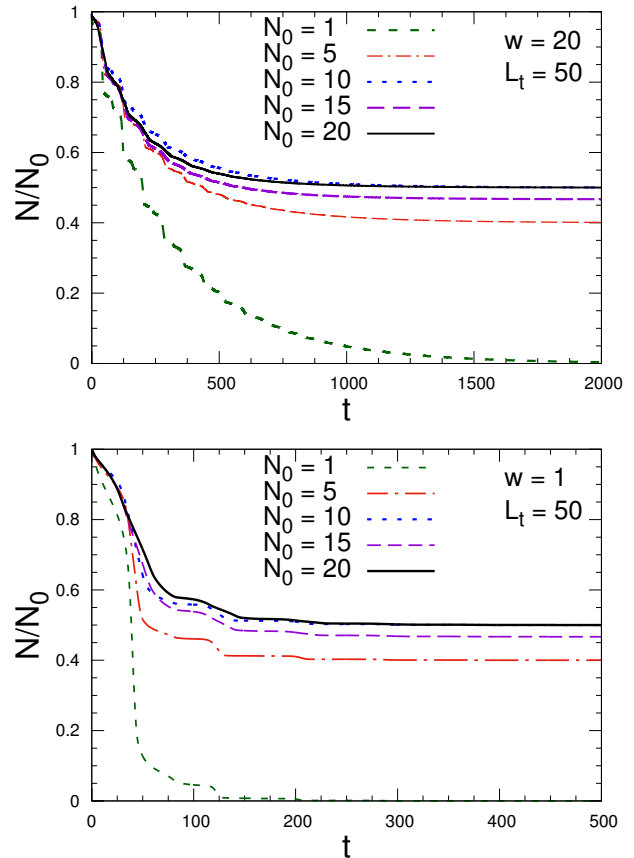


FIG. 14: The time dependence of the ratio N/N_0 for the central-site particle-loss dissipation $w = 1$ (bottom) and $w = 20$ (top) in systems within harmonic traps, various N_0 , and $L_t = 50$ (in the large- L limit to make the finite-size effects negligible). The asymptotic stationary limit turns out to converge to $N/N_0 = 1/2$ for even N_0 , and $N/N_0 = (N_0 - 1)/(2N_0)$ for odd N_0 . Similarly to the case of systems within hard walls, see Fig. 2, the approach to the asymptotic value turns out to be slower for $w = 20$ than $w = 1$.

We study the time evolution in the limit of large trap size L_t , in the case we keep the initial particle number N_0 fixed, and when we keep the ratio N_0/L_t constant (equivalent to adding a chemical potential). We consider harmonic traps, thus $p = 2$ in Eq. (3). The results are obtained for sufficiently large systems L at fixed L_t , so that a further increases of L does not change the results at fixed L_t , and therefore they can be considered as results for infinite-size systems with a large accuracy, within the accuracy of the numerical calculations, better than 10^{-8} .

A. Large-time behavior

To begin with, we discuss the asymptotic stationary states. In Fig. 14 we show the time dependence, and asymptotic behavior, of the ratio $N(t)/N_0$ for various

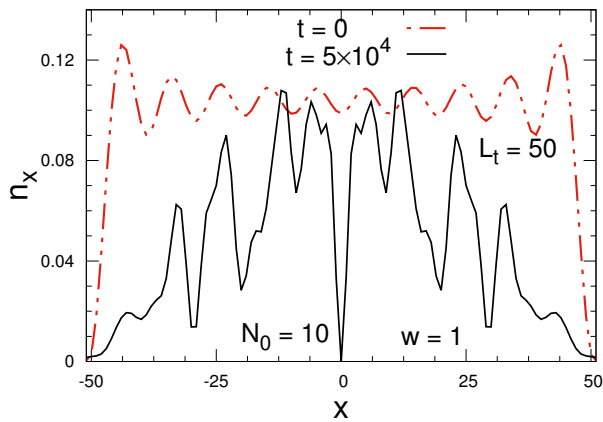


FIG. 15: The particle density n_x for systems within a harmonic trap with initial particle number $N_0 = 10$, at $t = 0$ and after some time t , for a central dissipation with $w = 1$, fixed trap size $L_t = 50$, and for a sufficiently large size of the system, $L = 221$, to make finite-size effects negligible (numerically checked by verifying the dependence on L).

values of the initial number of particles. Again, similarly to the case of homogeneous systems within hard walls and particle-decay dissipation at the center of the chain, we find that the large-time states keep a half of the initial particles. Analogously to the hard-wall case, this can be related to the fact that the one-particle Hamiltonian is invariant under reflections with respect to the center, thus the one-particle states must have definite parity. This can be easily seen in the continuum limit, see e.g. Ref. [67], where the one-particle Hamiltonian eigenfunctions can be written in terms of Hermite polynomials, and have definite parity. Since the one-particle states with negative parity vanishes at the center of the trap, the corresponding modes in the ground state of the fermionic system are not affected by the particle-decay dissipation at the center of the trap. Then, recalling that the ground state is obtained by filling the first N_0 one-particle levels, a selection mechanism analogous to that identified in the case of homogeneous systems applies, see Sec. III A, therefore half of them are odd [more precisely $N_0/2$ for even N_0 and $(N_0 - 1)/2$ for odd N_0], we expect again that half particles survive the central particle loss.

In Fig. 15 we show the particle density at $t = 0$ and at large time when the central particle density has already stably vanished. However, the spatial dependence of the particle density does not appear static in the large-time regime where the particle number stops decreasing. Indeed, as shown in Fig. 16, the time dependence of the particle density at sites $x \neq 0$ is characterized by time oscillations that apparently continue indefinitely, persisting even in the large- L_t limit. We also note that in this large-time regime the quantum evolution of the particle density appears effectively driven by the Hamiltonian term only. We have checked that the dissipative contribution in Eq. (10), i.e. the one proportional to w ,

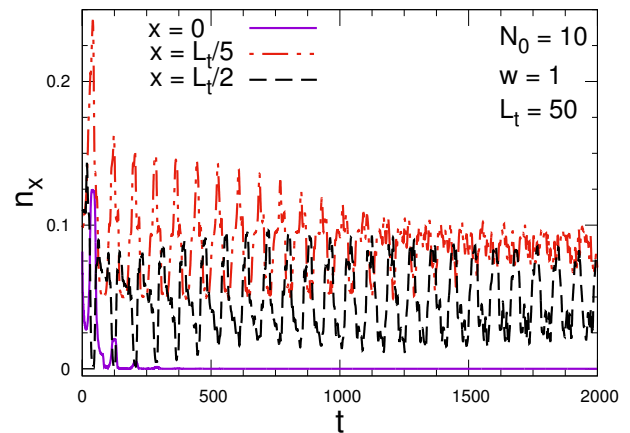


FIG. 16: Time dependence of the particle density for systems within a trap of size $L_t = 50$, at various spatial coordinates, $x = 0$, $x = L_t/5 = 10$ and $x = L_t/2 = 25$, for central dissipation with $w = 1$. The particle density n_x for $x \neq 0$ are characterized by oscillations in the large-time regime, when n_x at $x = 0$ and the particle number have already approached their asymptotic behavior.

gets suppressed asymptotically, thus only the Hamiltonian determines the large-time dependence of the fixed-time two-point function $\mathcal{C}_{xy}(t)$ and $n_x = \mathcal{C}_{xx}(t)$. In this large-time regime also the energy of the system defined in Eq. (13) remains constant, indeed its time derivative vanishes when $\text{Re } \mathcal{C}_{0,1} = 0$, cf. Eq. (15).

B. Large- L_t scaling behavior of the time dependence

The time dependence starting from a fixed number of particles shows the peculiar scaling behavior

$$R_N(t, w, L_t) \equiv \frac{N(t) - N_{\text{asy}}}{N_0 - N_{\text{asy}}} \approx A_t(t/L_t, w), \quad (31)$$

which apparently describes the whole time evolution. This is clearly supported by the data reported in Figs. 17 and 18 for central dissipation with $w = 1$ and initial particle number $N_0 = 10$.

Note that the time scale $t \sim L_t$ may be also related to the gap of the fermionic Hamiltonian, for which $\Delta_{L_t} \sim L_t^{-z\theta}$ where $z = 2$ is the dynamic exponent associated with the vacuum-to-superfluid transition, and $\theta = 1/2$ is the universal trap exponent characterizing critical behaviors in the presence of trapping potentials [23, 67, 69, 82] [for generic power laws of the potential (3), $\theta = p/(p+2)$].

The time scale $t \sim L_t$ characterizes the whole evolution of the system, up to the large-time regime, except for some small intermediate time intervals. Indeed, the curves shown in the bottom Fig. 17 presents some flat regions followed by rapid changes. Actually a more careful analysis, see, e.g., the top Fig. 17, shows that the scaling function $A_t(t/L_t, w)$ entering Eq. (31) ap-

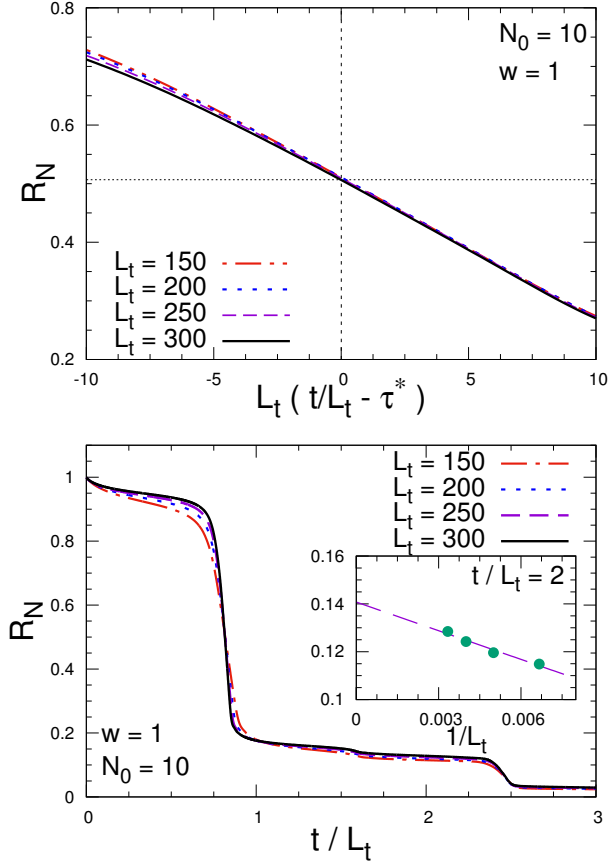


FIG. 17: The bottom figure shows the time evolution of the ratio R_N versus t/L_t for $w = 1$, various trap sizes, keeping the initial number of particles $N_0 = 10$ fixed. The inset shows an example of convergence at $t/L_t = 2$. The top figure shows the scaling behavior at the fast drop of the particle number, around $t/L_t \approx 0.8147$, described by Eq. (32).

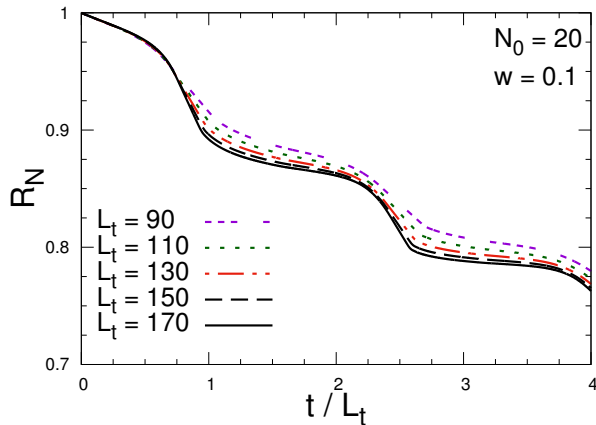


FIG. 18: The ratio R_N for $w = 0.1$, various trap sizes, keeping the initial number of particles $N_0 = 20$ fixed.

pears to develop a singularity in the large-time limit, at

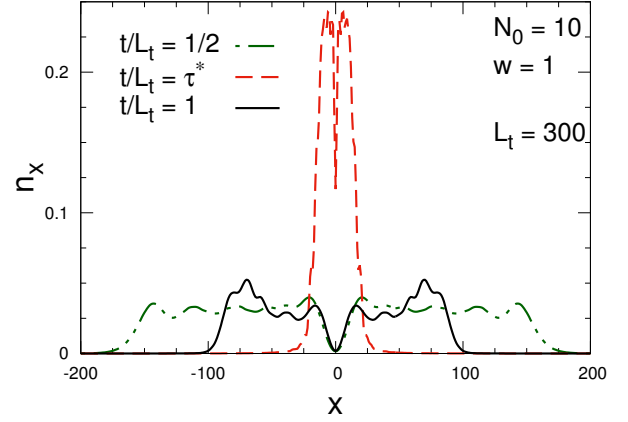


FIG. 19: Behavior of the particle density around the singularity of the scaling function (31), for $L_t = 300$, central particle loss with $w = 1$, and some values of the ratio t/L_t around the singular point $t/L_t = \tau^* \approx 0.8147$. They show that large drop of the particle number at τ^* is connected with a simultaneous large increase of the particle density at the center of the trap.

$t/L_t = \tau^* \approx 0.8147$, so that

$$A_t(t/L_t, w) \approx f[L_t(t/L_t - \tau^*)] \quad (32)$$

around $t/L_t = \tau^*$. Therefore this sharp drop of the particle density occurs at a time $t^* \approx L_t \tau^*$ in the large- L_t limit, and lasts for a finite time interval, i.e. it does not diverge when increasing L_t . Some data for the behavior of the particle density and number around the time τ^* are shown in Fig. 19, where we note the significant increase of the particle density around $x = 0$ when the singular behavior of the scaling function (31) appears. Analogous behaviors are observed for generic values of N_0 and w .

In the case we keep N_0/L_t fixed, the results show a generic scaling behavior in terms of t/L_t , analogous to Eq. (31), see for example Fig. 20.

V. SUMMARY AND CONCLUSIONS

We have addressed the out-of-equilibrium dynamics of fermionic gases confined within finite spatial regions, subject to localized dissipative interactions with the environment, entailing a localized loss of particles. We consider systems where particles are constrained within a limited spatial region by hard walls, and systems where they are trapped by a space-dependent potential, such as an effective harmonic potential. These issues are particularly relevant for cold-atom experiments, where atoms are confined within a limited spatial region by external potentials [54]. Within this class of confined particle systems, we investigate the dynamic features arising from localized particle-loss dissipative mechanisms, which may be controllable, or inevitably present, in the experimental setup. We discuss the quantum evolution at small and

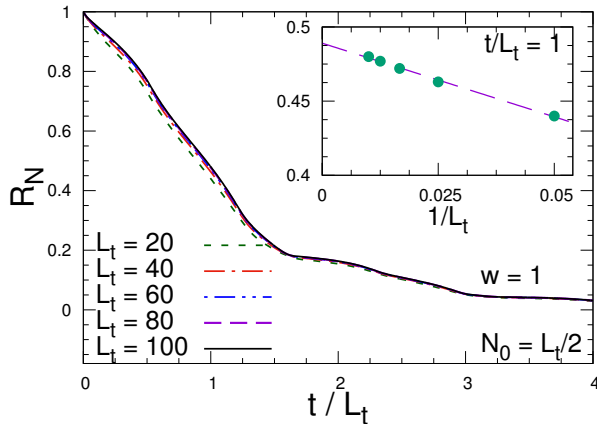


FIG. 20: Time evolution of the ratio R_N versus t/L_t for fermionic gases within harmonic traps of various size, keeping the ratio $N_0/L_t = 1/2$ fixed, for central particle-loss dissipation with $w = 1$. The large- L_t convergence is evident, as also shown by the plot reported within the inset.

large times, focussing on the effects of finiteness of the confining region, which becomes eventually relevant for sufficiently large times.

As paradigmatic models we consider one-dimensional non-interacting spinless fermionic lattice gases within hard-wall and harmonic traps, with a particle loss localized at one of the sites of the chain, for example at the center of the system, as sketched in Fig. 1. The dissipative particle-decay mechanism is modeled within the framework of the Lindblad master equation governing the time evolution of the density matrix. Such a dissipative quantum dynamics is analyzed within protocols starting from the equilibrium ground state of the fermionic gas, then evolving under the effect of the particle-loss dissipation, as outlined in Sec. II C.

We mostly exploit dynamic FSS frameworks, based on the definition of appropriate large-size limits. This approach allows us to characterize the dynamics in the presence of localized particle-loss dissipation, identifying different dynamic regimes related to different features of the dissipative system, whose time scales are associated with powers of the size ℓ .

The interplay between the time dependence and the size ℓ of the system (ℓ corresponds to M where $L = 2M + 1$ for hard-wall confinement, and the trap size L_t , cf. Eq. (3), for inhomogeneous potential traps) is studied for two different initial conditions: (i) fixed number N_0 of initial particles; (ii) keeping the ratio N_0/ℓ constant, corresponding to the *thermodynamic* limit of the initial fermionic gases at equilibrium, in both hard walls and harmonic traps. These protocols provide us with complementary information on the actual dynamics of finite-size systems with relatively large size. The time dependence of the particle number and density show various dynamic scaling regimes in the large-size limit, and non-trivial asymptotic large-time behaviors. Notable differ-

ences emerge between homogeneous systems within hard walls and systems within inhomogeneous harmonic traps.

The quantum evolution, arising from the dynamic protocol that we consider, leads to asymptotic trivial empty states for generic locations of the localized dissipative interaction. However there are notable exceptions, in particular when the particle loss is localized at the center of the system, in both hard-wall and harmonic traps. In this case only a fraction of the particles eventually disappears, while half of them survives. This is essentially related to the non-interacting nature of the fermionic gases, so that the localized dissipative mechanism preserves the particle modes associated with the one-particle wave functions that vanish at the site where the particle loss occurs, see Sec. III A. Therefore, due to the invariance under inversion with respect to the center of the system, half one-particle modes vanish at the center of the trap, thus they do not suffer from particle loss. The particle density at the site of the dissipation vanishes for sufficiently large time. When this happens the particle number $N(t)$ stops decreasing, cf. Eq. (12), then the residual particle number remains constant, because the localized dissipative mechanism cannot reduce the particle number anymore. This shows that there are two main different dynamic regimes in the presence of one central particle-loss defect: the quantum dynamics is initially driven by the particle-loss dissipation until the central particle density gets asymptotically suppressed, then the subsequent large-time evolution conserves the particle number and energy.

In the case of non-interacting fermionic gases confined within hard walls, of size $L = 2M + 1$, the out-of-equilibrium evolution arising from the protocol considered shows various dynamic regimes, which can be effectively distinguished by relating them to dynamic FSS limits corresponding to different time scales, which can be associated with the gap of the Liouvillian gap of the Lindblad equation, and the gap of its Hamiltonian driving. The main features of the out-of-equilibrium evolution can be summarized as follows.

(i) The asymptotic large-time states are characterized by a residual number $N_{\text{asy}} = N(t \rightarrow \infty)$ of particles: $N_{\text{asy}} = N_0/2$ for even N_0 , and $N_{\text{asy}} = (N_0 - 1)/2$ for odd N_0 . Also the particle density $n_x(t)$ shows a large-time stationary (time independent) condition, with an almost constant n_x , except at $x = 0$ where it vanishes.

(ii) The approach to the asymptotic stationary states is controlled by the Liouvillian gap (22), which decreases as L^{-3} asymptotically. Therefore, for generic dissipative couplings w , the times scale of the approach to the stationary state behaves as $t_a \sim L^3$. Correspondingly, the particle-number ratio R_N defined in Eq. (26) shows the asymptotic scaling behavior $R_N(t, w, L) \approx A(t/L^3, w)$.

(iii) When we consider the large-size limit keeping the initial number N_0 of particle fixed, the quantum evolution shows another intermediate dynamic regime, i.e. $R_N \approx U(t/L^2, wL)$ which is obtained in the large- L limit by keeping t/L^2 and wL fixed. This regime may be as-

sociated with the gap of the Hamiltonian driving, which behaves as $\Delta_H \sim L^{-2}$.

(iv) Different intermediate regimes are observed when we keep N_0/M fixed (equivalent to N_0/L fixed) in the large-size limit. We observe an intermediate dynamic scaling behavior $R_N \approx W(t/L, w)$, which can be related to the size-dependence $\Delta_s \sim 1/L$ of the Hamiltonian gap when the ratio N_0/L is kept fixed.

(v) When N_0/M is kept fixed, there is also a further early time regime, where the particle-number derivative depends only on time, without showing any dependence on the size [43]. This may be considered as the *thermodynamic* limit of the dynamics arising from the protocol. Of course, this early-time regime stops when the particle dynamics starts becoming sensitive to the boundaries, i.e. for times $t \sim L$.

Substantially different behaviors emerge when we consider fermionic gases trapped by an inhomogeneous harmonic potential within a region of size L_t , cf. Eq. (3). We again consider the dynamic in the case of one central particle-loss defect, whose main features can be summarized as follows.

(i) The large-time behavior is again characterized by a residual number of particles, analogously to the hard-wall case. The large-time behavior of the particle density is again characterized by the vanishing of n_x at the dissipation site $x = 0$, so that the particle number stops decreasing. However the behavior of particle density n_x at $x \neq 0$ is not static in this large-time regime. Indeed it shows sizable oscillations in time for $x \neq 0$, without apparently reaching an asymptotic static condition, at least for finite trap sizes. We also note that, when the particle density at the central site reaches its asymptotic zero value in the large-time regime, the time evolution becomes effectively unitary for the particle density n_x , i.e. it matches the behavior due to the only unitary driving in the Lindblad equation, and conserves the energy.

(ii) The approach to the large-time behavior where $N(t)$ stops decreasing is essentially characterized by time scales $t_a \sim L_t$. This gives rise to the dynamic scaling behavior $R_N \approx A_t(t/L_t, w)$ in the large- L_t limits, in both cases when keeping N_0 or N_0/L_t fixed. We also mention that, in the case of a fixed initial particle number N_0 , the scaling function $A_t(t/L_t, w)$ shows intervals of t/L_t with an almost flat (slowly decreasing) dependence and apparent singularities between them, where the particle number drops significantly in a small time scale independent of L_t .

A natural extension of the study reported here may be that of considering interacting fermionic systems, such as the Hubbard model. Some results for interacting homogeneous fermionic systems have been already reported in Refs. [35, 42, 43], mostly discussing infinite-size properties. Analogously to what done in this paper for free fermionic gases, we believe that it is worth studying the complex dynamic phenomena arising from the presence of the boundaries, or inhomogeneous external trapping potential, even in the case of interacting particle systems. Of course, the analysis of interacting systems becomes significantly more challenge. Numerical methods

to investigate interacting particle systems may be based on the so-called quantum trajectory algorithms, which sample different quantum trajectories driven by an effective Hamiltonian and stochastic quantum jumps, see e.g. Refs. [32, 43]. Other possible extensions of our work may consider different types of localized dissipative mechanisms, and also higher dimensional systems.

We finally remark that the comprehension of the interplay between the time dependence and the finite size of the confined system is essential to interpret the behavior of physical systems when boundary effects become important. For example this issue is relevant for small-size quantum simulators operating on a limited amount of quantum objects, in the presence of controlled dissipation. We also mention experiments with cold atoms within a trap of finite size, when the many-body correlations become eventually sensitive to the inhomogeneity arising from the trapping potential.

Appendix A: Liouvillian gap

To compute the Liouvillian gap for systems within hard walls, we follow the method outlined in Ref.[26]. As explained there, the results are obtained by diagonalization of the $4L \times 4L$ anti-symmetric complex matrix A with nonzero elements ($j, k = -2M - 1, \dots, 2M$ and $L = 2M + 1$)

$$\begin{aligned} A_{2j-1, 2k-1} &= -2iH_{jk} - D_{jk}/2 + D_{kj}/2, \\ A_{2j-1, 2k} &= iD_{kj}, \\ A_{2j, 2k-1} &= -iD_{jk}, \\ A_{2j, 2k} &= -2iH_{jk} + D_{jk}/2 - D_{kj}/2, \end{aligned} \quad (\text{A1})$$

where the dissipation $2L \times 2L$ matrix $D_{j,k}$ describes the effects of localized particle-loss dissipation at the central site,

$$D_{j,k} = l_j l_k^*, \quad l_j = \frac{w}{2} (\delta_{j,-2} - i \delta_{j,-1}), \quad (\text{A2})$$

and the $(2L, 2L)$ matrix $H_{j,k}$ is associated with the Hamiltonian (1) written in terms of the Majorana fermion operators $\{v_j\}$,

$$\begin{aligned} \hat{H} &= \sum_{jk} \hat{v}_j H_{jk} \hat{v}_k = -\frac{1}{4} \sum_{j=-M}^M \left(i \hat{v}_{2j-1} \hat{v}_{2j} - \right. \\ &\quad \left. - i \hat{v}_{2j} \hat{v}_{2j+1} + i \hat{v}_{2j-1} \hat{v}_{2j+2} + \text{h.c.} \right), \end{aligned} \quad (\text{A3})$$

with ($x = -M, \dots, M$):

$$\hat{v}_{2x} = \hat{c}_x + \hat{c}_x^\dagger, \quad \hat{v}_{2x-1} = i(\hat{c}_x^\dagger - \hat{c}_x). \quad (\text{A4})$$

If β_j are the eigenvalues of the matrix A , then the Liouvillian gap is given by

$$\Delta_{\mathcal{L}} = 2 \text{Min} [\text{Re} \beta_j]. \quad (\text{A5})$$

-
- [1] I. Bloch, Quantum coherence and entanglement with ultracold atoms in optical lattices, *Nature* **453**, 1016 (2008).
- [2] I. M. Georgescu, S. Ashhab, and F. Nori, Quantum simulation, *Rev. Mod. Phys.* **86**, 153 (2014).
- [3] A. A. Houck, H. E. Türeci, and J. Koch, On-chip quantum simulation with superconducting circuits, *Nat. Phys.* **8**, 292 (2012).
- [4] M. Müller, S. Diehl, G. Pupillo, and P. Zoller, Engineered open systems and quantum simulations with atoms and ions, *Adv. At. Mol. Opt. Phys.* **61**, 1 (2012).
- [5] H. Ritsch, P. Domokos, F. Brennecke, and T. Esslinger, Cold atoms in cavity-generated dynamical optical potentials, *Rev. Mod. Phys.* **85**, 553 (2013).
- [6] I. Carusotto and C. Ciuti, Quantum fluids of light, *Rev. Mod. Phys.* **85**, 299 (2013).
- [7] M. Aspelmeyer, T. J. Kippenberg, and F. Marquardt, Cavity optomechanics, *Rev. Mod. Phys.* **86**, 1391 (2014).
- [8] A. J. Daley, Quantum trajectories and open many-body quantum systems, *Adv. Phys.* **63**, 77 (2014).
- [9] L. M. Sieberer, M. Buchhold, and S. Diehl, Keldysh field theory for driven open quantum systems, *Rep. Prog. Phys.* **79**, 096001 (2016).
- [10] M. J. Hartmann, Quantum simulation with interacting photons, *J. Opt.* **18**, 104005 (2016).
- [11] C. Noh and D. G. Angelakis, Quantum simulations and many-body physics with light, *Rep. Prog. Phys.* **80**, 016401 (2017).
- [12] F. Minganti, A. Biella, N. Bartolo, and C. Ciuti, Spectral theory of Liouvillians for dissipative quantum transitions, *Phys. Rev. A* **98**, 042118 (2018).
- [13] Y. Li, X. Chen, and M. P. A. Fisher, Measurement-driven entanglement transition in hybrid quantum circuits, *Phys. Rev. B* **100**, 134306 (2019).
- [14] B. Skinner, J. Ruhman, and A. Nahum, Measurement-induced phase transitions in the dynamics of entanglement, *Phys. Rev. X* **9**, 031009 (2019).
- [15] S. Yin, P. Mai, and F. Zhong, Nonequilibrium quantum criticality in open systems: The dissipation rate as an additional indispensable scaling variable, *Phys. Rev. B* **89**, 094108 (2014).
- [16] S. Yin, C.-Y. Lo, and P. Chen, Scaling behavior of quantum critical relaxation dynamics of a system in a heat bath, *Phys. Rev. B* **93**, 184301 (2016).
- [17] D. Nigro, D. Rossini, and E. Vicari, Competing coherent and dissipative dynamics close to quantum criticality, *Phys. Rev. A* **100**, 052108 (2019).
- [18] D. Rossini and E. Vicari, Scaling behavior of stationary states arising from dissipation at continuous quantum transitions, *Phys. Rev. B* **100**, 174303 (2019).
- [19] D. Rossini and E. Vicari, Dynamic Kibble-Zurek scaling framework for open dissipative many-body systems crossing quantum transitions, *Phys. Rev. Research* **2**, 023211 (2020).
- [20] G. Di Meglio, D. Rossini, and E. Vicari, Dissipative dynamics at first-order quantum transitions, *Phys. Rev. B* **102**, 224302 (2020).
- [21] L. Rosso, D. Rossini, A. Biella, and L. Mazza, One-dimensional spin-1/2 fermionic gases with two-body losses: weak dissipation and spin conservation, *Phys. Rev. A* **104**, 053305 (2021).
- [22] V. Alba and F. Carollo, Hydrodynamics of quantum entropies in Ising chains with linear dissipation, *J. Phys. A: Math. Theor.* **55**, 074002 (2022).
- [23] D. Rossini and E. Vicari, Coherent and dissipative dynamics at quantum phase transitions, *Phys. Rep.* **936**, 1 (2021).
- [24] R. Livi, R. Franzosi, and G. Oppo, Self-Localization of Bose-Einstein Condensates in Optical Lattices via Boundary Dissipation, *Phys. Rev. Lett.* **97**, 060401 (2006).
- [25] T. Prosen and I. Pizorn, Quantum Phase Transition in a Far-from-Equilibrium Steady State of an XY Spin Chain, *Phys. Rev. Lett.* **101**, 105701 (2008).
- [26] T. Prosen, Third quantization: a general method to solve master equations for quadratic open Fermi systems, *New J. Phys.* **10**, 043026 (2008).
- [27] D. Witthaut, F. Trimborn, and S. Wimberger, Dissipation Induced Coherence of a Two-Mode Bose-Einstein Condensate, *Phys. Rev. Lett.* **101**, 200402 (2008).
- [28] D. Witthaut, F. Trimborn, H. Hennig, G. Kordas, T. Geisel, and S. Wimberger, Beyond mean-field dynamics in open Bose-Hubbard chains, *Phys. Rev. A* **83**, 063608 (2011).
- [29] K. V. Kepesidis and M. J. Hartmann, Bose-Hubbard model with localized particle losses, *Phys. Rev. A* **85**, 063620 (2012).
- [30] G. Kordas, S. Wimberger, and D. Witthaut, Decay and fragmentation in an open Bose-Hubbard chain, *Phys. Rev. A* **87**, 043618 (2013).
- [31] L. Bianchi, P. Giorda, and P. Zanardi, Quantum information-geometry of dissipative quantum phase transitions, *Phys. Rev. E* **89**, 022102 (2014).
- [32] G. Kordas, D. Witthaut, P. Buonsante, A. Vezzani, R. Burioni, A.I. Karanikas, and S. Wimberger, The dissipative Bose-Hubbard model, *Eur. Phys. J ST* **224**, 2127 (2015).
- [33] M. Znidaric, Relaxation times of dissipative many-body quantum systems, *Phys. Rev. E* **92**, 042143 (2015).
- [34] L. M. Vasiloiu, F. Carollo, and J. P. Garrahan, Enhancing correlation times for edge spins through dissipation, *Phys. Rev. B* **98**, 094308 (2018).
- [35] H. Fröml, A. Ciocchetta, C. Kollath, and S. Diehl, Fluctuation-Induced Quantum Zeno Effect, *Phys. Rev. Lett.* **122**, 040402 (2019).
- [36] M. Lebrat, S. Häusler, P. Fabritius, D. Husmann, L. Corman, and T. Esslinger, Quantized conductance through a spin-selective atomic point contact, *Phys. Rev. Lett.* **123**, 193605 (2019).
- [37] F. Tonielli, R. Fazio, S. Diehl, and J. Marino, Orthogonality catastrophe in dissipative quantum many body systems, *Phys. Rev. Lett.* **122**, 040604 (2019).
- [38] W. Berdanier, J. Marino, and E. Altman, Universal Dynamics of Stochastically Driven Quantum Impurities, *Phys. Rev. Lett.* **123**, 230604 (2019).
- [39] P. L. Krapivsky, K. Mallick, and D. Sels, Free fermions with a localized source, *J. Stat. Mech.* (2019) 113108.
- [40] N. Shibata and H. Katsura, Dissipative spin chain as a non-Hermitian Kitaev ladder, *Phys. Rev. B* **99**, 174303 (2019).
- [41] N. Shibata and H. Katsura, Quantum Ising chain with boundary dephasing, *Prog. Theor. Exp. Phys.* **12A108**

- (2020).
- [42] S. Wolff, A. Sheikhan, S. Diehl, and C. Kollath, Non-equilibrium metastable state in a chain of interacting spinless fermions with localized loss, *Phys. Rev. B* **101**, 075139 (2020).
- [43] H. Fröml, C. Muckel, C. Kollath, A. Chiocchetta, and S. Diehl, Ultracold quantum wires with localized losses: many-body quantum Zeno effect, *Phys. Rev. B* **101**, 144301 (2020).
- [44] T. Mori and T. Shirai, Resolving a Discrepancy between Liouvillian Gap and Relaxation Time in Boundary-Dissipated Quantum Many-Body Systems, *Phys. Rev. Lett.* **125**, 230604 (2020).
- [45] P. E. Dolgirev, J. Marino, D. Sels and E. Demler, Non-Gaussian correlations imprinted by local dephasing in fermionic wires, *Phys. Rev. B* **102**, 100301(R) (2020).
- [46] G. Amato, H.-P. Breuer, S. Wimberger, A. Rodriguez, and A. Buchleitner, Non-interacting many-particle quantum transport between finite reservoirs, *Phys. Rev. A* **102**, 022207 (2020).
- [47] D. Rossini, A. Ghermaoui, M. Bosch Aguilera, R. Vatrè, R. Bouganne, J. Beugnon, F. Gerbier, and L. Mazza, Strong correlations in lossy one-dimensional quantum gases: from the quantum Zeno effect to the generalized Gibbs ensemble, *Phys. Rev. A* **103**, L060201 (2021).
- [48] F. Tarantelli and E. Vicari, Quantum critical systems with dissipative boundaries, *Phys. Rev. B* **104**, 075140 (2021).
- [49] V. Alba and F. Carollo, Noninteracting fermionic systems with localized dissipation: Exact results in the hydrodynamic limit, *Phys. Rev. B* **105**, 054303 (2022).
- [50] A. Nava, M. Rossi, and D. Giuliano, Lindblad equation approach to the determination of the optimal working point in nonequilibrium stationary states of an interacting electronic one-dimensional system: Application to the spinless Hubbard chain in the clean and in the weakly disordered limit, *Phys. Rev. B* **103**, 115139 (2021).
- [51] P. Würtz, T. Langen, T. Gericke, A. Koglbauer, and H. Ott, Experimental Demonstration of Single-Site Addressability in a Two-Dimensional Optical Lattice, *Phys. Rev. Lett.* **103**, 080404 (2009).
- [52] R. Labouvie, B. Santra, S. Heun, S. Wimberger and H. Ott, Negative Differential Conductivity in an Interacting Quantum Gas, *Phys. Rev. Lett.* **115**, 050601 (2015).
- [53] R. Labouvie, B. Santra, S. Heun, and H. Ott, Bistability in a Driven-Dissipative Superfluid, *Phys. Rev. Lett.* **116**, 235302 (2016).
- [54] I. Bloch, J. Dalibard, and W. Zwerger, Many-body physics with ultracold gases, *Rev. Mod. Phys.* **80**, 885 (2008).
- [55] A. L. Gaunt, T. F. Schmidutz, I. Gotlibovych, R. P. Smith and Z. Hadzibabic, Bose-Einstein condensation of atoms in a uniform potential, *Phys. Rev. Lett.* **110**, 200406 (2013).
- [56] V. Privman, Finite size scaling and numerical simulation of statistical systems, World Scientific (Singapore, 1990).
- [57] J. Cardy, *Scaling and renormalization in statistical physics*, Cambridge University Press, 1996.
- [58] A. Pelissetto and E. Vicari, Critical Phenomena and Renormalization Group Theory, *Phys. Rep.* **368**, 549 (2002).
- [59] G. Lindblad, On the generators of quantum dynamical semigroups, *Commun. Math. Phys.* **48**, 119 (1976).
- [60] V. Gorini, A. Kossakowski, and E. C. G. Sudarshan, Completely positive dynamical semigroups of N-level systems, *J. Math. Phys.* **17**, 821 (1976).
- [61] H.-P. Breuer and F. Petruccione, *The Theory of Open Quantum Systems* (Oxford University Press, New York, 2002).
- [62] A. Rivas and S. F. Huelga, *Open Quantum System: An Introduction* (SpringerBriefs in Physics, Springer, 2012).
- [63] A. D’Abbruzzo and D. Rossini, Self-consistent microscopic derivation of Markovian master equations for open quadratic quantum systems, *Phys. Rev. A* **103**, 052209 (2021).
- [64] G. Ceccarelli, C. Torrero, and E. Vicari, Critical parameters from trap-size scaling in trapped particle systems, *Phys. Rev. B* **87**, 024513 (2013).
- [65] M. Rigol and A. Muramatsu, Universal properties of hard-core bosons confined on one-dimensional lattices, *Phys. Rev. A* **70**, 031603(R) (2004).
- [66] M. Campostrini and E. Vicari, Quantum critical behavior and trap-size scaling of trapped bosons in a one-dimensional optical lattice, *Phys. Rev. A* **81**, 063614 (2010).
- [67] A. Angelone, M. Campostrini, E. Vicari, Universal quantum behaviors of interacting fermions in 1D traps: from few particles to the trap thermodynamic limit, *Phys. Rev. A* **89**, 023635 (2014).
- [68] D. Nigro, Trap effects and the continuum limit of the Hubbard model in the presence of a harmonic potential, *Phys. Rev. A* **96**, 033608 (2017).
- [69] M. Campostrini and E. Vicari, Trap-size scaling in confined particle systems at quantum transitions, *Phys. Rev. A* **81**, 023606 (2010).
- [70] M. Campostrini and E. Vicari, Equilibrium and off-equilibrium trap-size scaling in 1D ultracold bosonic gases, *Phys. Rev. A* **82**, 063636 (2010).
- [71] M. Campostrini and E. Vicari, Bipartite quantum entanglement of one-dimensional lattice systems with a trapping potential, *J. Stat. Mech.: Theory Exp.* (2010) P08020; (2011) E04001 (E).
- [72] L. Pollet, Recent developments in quantum Monte Carlo simulations with applications for cold gases, *Rep. Prog. Phys.* **75**, 094501 (2012).
- [73] E. Vicari, Entanglement and particle correlations of Fermi gases in harmonic traps, *Phys. Rev. A* **85**, 062104 (2012).
- [74] P. Calabrese, P. Le Doussal, and S. N. Majumdar, Random matrices and entanglement entropy of trapped Fermi gases, *Phys. Rev. A* **91**, 012303 (2015).
- [75] B. Horstmann and J. I. Cirac, Noise-driven dynamics and phase transitions in fermionic systems, *Phys. Rev. A* **87**, 012108 (2013).
- [76] M. Keck, S. Montangero, G. E. Santoro, R. Fazio, and D. Rossini, Dissipation in adiabatic quantum computers: lessons from an exactly solvable model, *New. J. Phys.* **19**, 113029 (2017).
- [77] D. Nigro, On the uniqueness of the steady-state solution of the Lindblad-Gorini-Kossakowski-Sudarshan equation, *J. Stat. Mech.* (2019) 043202.
- [78] S. Sachdev, *Quantum Phase Transitions*, (Cambridge University, Cambridge, England, 1999).
- [79] B. Misra, E. C. G. Sudarshan, The Zeno’s paradox in quantum theory. *J. Math. Phys.* **18**, 756 (1977).
- [80] P. Facchi and S. Pascazio, Quantum Zeno dynamics: Mathematical and physical aspects, *J. Phys. A: Math. Theor.* **41**, 493001 (2008).

- [81] T. Tomita, S. Nakajima, I. Danshita, Y. Takasu, and Y. Takahashi, Observation of the Mott insulator to superfluid crossover of a driven-dissipative Bose-Hubbard system, *Adv.* **3**, e1701513 (2017).
- [82] M. Campostrini and E. Vicari, Critical behavior and scaling in trapped systems, *Phys. Rev. Lett.* **102**, 240601 (2009); *Phys. Rev. Lett. (E)* **103**, 269901 (2009).